

Magnetic Structure of Fe₅O₆: Group-Theoretical Analysis and DFT Calculations

V. S. Zhandun^{a, b, *}, N. V. Kazak^a, and D. M. Vasiukov^{c, d}

^a Kirensky Institute of Physics, Federal Research Center KSC, Siberian Branch, Russian Academy of Sciences, Krasnoyarsk, 660036 Russia

^b Krasnoyarsk State Medical University named after Professor L.F. Voino-Yasenetsky, Krasnoyarsk, 660022 Russia

^c Division of Synchrotron Radiation Research, Department of Physics, Lund University, Lund, 221 00 Sweden

^d Materials Science and Applied Mathematics, Malmö University, Malmö, 204 06 Sweden

*e-mail: jvc@iph.krasn.ru

Received November 22, 2023; revised December 26, 2023; accepted December 29, 2023

The magnetic structure of Fe₅O₆ is studied using a combination of the group-theoretical analysis and DFT + *U* calculations of the electronic spectrum. The calculations are performed for the magnetic $\mathbf{k} = (0, 0, 0)$ vector. The magnetic ground state corresponds to the orthogonal ordering of two magnetic subsystems: the magnetic moments of Fe²⁺/Fe³⁺ ions located at the octahedral sites (slabs of octahedra) are directed along the *c* axis and are antiferromagnetically ordered, whereas the magnetic moments of Fe²⁺ ions in trigonal prisms forming one-dimensional chains are directed along the *b* axis and are antiferromagnetically coupled along the *c* axis. The formation of a nonzero antiferromagnetic component of magnetic moments in the slabs of octahedra directed along the *b* axis is caused by the effect of magnetic chains on the three-dimensional magnetic structure.

DOI: 10.1134/S0021364023604244

1. INTRODUCTION

The crystal chemistry and physical properties of novel high-pressure iron oxides forming the homologous series $n\text{FeO} \cdot m\text{Fe}_2\text{O}_3$ (Fe₄O₅, Fe₅O₆, Fe₅O₇, etc.) have been of great interest since their discovery [1–14]. The crystal structure of these oxides involves two basic building blocks: FeO₆ oxygen octahedra connected by common edges form slabs separated by chains of prismatically coordinated Fe ions. Some representatives of this series of oxides are stable at atmospheric pressure, which allows performing a thorough analysis of their physical properties [3, 7]. These oxides are mixed valence compounds, exhibiting anomalies in the electrical resistivity related to charge ordering [3, 7] and phase transitions similar to the Verwey transition [15].

A unified approach for treating these oxides based on the generating crystallographic mechanism of this homologous series was recently proposed in [12]. It turned out that the regular twinning of the wüstite (FeO) structure by the mirror plane at the unit cell scale can generate the whole variety of crystal structures of this series. The periodicity or, in other words, the cycle of this twinning is the key factor that determines the symmetry, stoichiometry, and oxidation state of the generated structures, and naturally divides the homological series into two subgroups: the orthor-

hombic *N* family and the monoclinic *N*, *N* + 1 family [12]. The first family is based on a simple monomial cycle, i.e., the repetition of a single slab consisting of *N* octahedra, such as $\eta\text{-Fe}_2\text{O}_3$, HP-Fe₃O₄, Fe₄O₅, and Fe₅O₆ with *N* = 1, 2, 3, and 4, respectively. The second family is based on a binomial cycle; i.e., the structures are generated by alternating slabs of different widths, *N* and *N* + 1, and include Fe₅O₇, Fe₇O₉, and Fe₉O₁₁ oxides. A generic magnetic structure with collinear subsystems of octahedral slabs and chains ordered orthogonally with respect to each other has been put forward for the *N*-family [12]. The resulting magnetic structure will be ferromagnetic or antiferromagnetic if *N* is odd or even, respectively.

To date, the most well-studied oxides are orthorhombic ones with *N* = 3. Numerous magnetic measurements and neutron diffraction data for the magnetic structure of a number of isostructural oxides Me²⁺Fe₃O₅, in which prismatic sites are occupied by divalent ions such as Mn, Co, and Ca have demonstrated that a collinear antiferromagnetic spin order appears in the slabs of octahedra near 300 K and magnetic moments are directed along the *c* axis, whereas a ferromagnetic spin order in chains along the *b* axis occurs independently at much lower temperatures of ~100 K [16–19].

The magnetic structure of oxides with $N = 3$ was theoretically studied in our previous work [20] using a comprehensive approach combining the group-theoretical analysis of possible magnetic structures and a subsequent analysis (density functional theory) DFT calculation of the energies of these structures. For Fe₄O₅, it was shown that the magnetic phase with $k = (0, 0, 0)$, which is characterized by ferromagnetic ordering of iron moments at the prismatic sites along the b axis and antiferromagnetic ordering of iron moments at the octahedral sites along the c axis, has the lowest energy [20]. Thus, the ground magnetic state corresponds to the orthogonal spin order and is consistent with the magnetic structure proposed in [12]. However, the aspect of the conjecture that concerns the change of the ferromagnetic state to the antiferromagnetic one when the slab width changes from odd to even N remains unconfirmed.

This study concerns Fe₅O₆ with $N = 4$. Measurements of the magnetic susceptibility of this oxide demonstrated that the material exhibits an antiferromagnetic transition at $T_N = 100$ K [7]. Low-temperature measurements ($T < T_N$) revealed anomalies in the magnetic field dependences of the magnetization due to the transformation of the antiferromagnetic subsystem in an applied field. The Mössbauer spectra measured at room temperature and atmospheric pressure are approximated by the sum of two components: a paramagnetic doublet associated with Fe²⁺ ions in the prismatic environment and a magnetic sextet assigned to Fe²⁺/Fe³⁺ ions in the octahedral environment, which corresponds to the ratio of the areas of the spectral components $A(\text{Fe}^{\text{pr}}):A(\text{Fe}^{\text{oct}}) = 0.19:0.81$ [12]. Thus, the available magnetic data on Fe₅O₆ suggest that the magnetically ordered and disordered subsystems coexist at room temperature.

In the present work, the magnetic structure of Fe₅O₆ is studied using the group-theoretical analysis of irreducible representations and DFT calculations.

2. CALCULATION METHODS

The DFT calculations were performed with the VASP [21] using the RAW pseudopotentials [22], the PBE parameterization of the exchange-correlation functional, and the generalized gradient approximation [23]. The valence configurations $3d^64s^2$ and $2s^22p^2$ were used for the Fe and O atoms, respectively. The spin-orbit coupling was included in all DFT-GGA calculations. The cutoff energy for the plane wave was 500 eV. We used the $11 \times 4 \times 3$ Monkhorst-Pack grids of special points to integrate over the Brillouin zone [24]. The energy convergence criteria were 10^{-5} and 10^{-4} eV for electron and ion relaxation, respectively. We employed the GGA+ U approach in the Dudarev approximation [25] and the Coulomb parameter $U = 3.2$ eV for the best agreement between the experimental [7] and theoretical values of the band gap width.

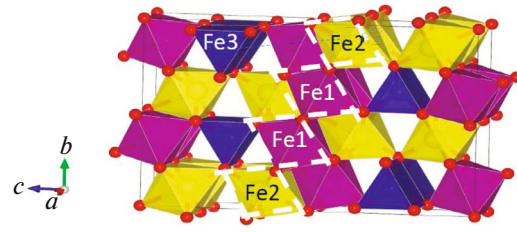


Fig. 1. (Color online) Crystal structure of Fe₅O₆. Symmetry-inequivalent iron atoms Fe1, Fe2, and Fe3 are shown in purple, yellow, and blue, respectively. The dashed line highlights a slab of octahedra with $N = 4$. All pictures of crystal and magnetic structures in this work were created using the VESTA software [27].

The BASIREPS program [26] was used to construct magnetic configurations with the propagation vector $\mathbf{k} = (0, 0, 0)$.

3. RESULTS AND DISCUSSION

The Fe₅O₆ iron oxide has an orthorhombic unit cell (space group $Cmcm$), which contains four formula units and three symmetry-inequivalent iron sites (Fig. 1). Two iron atoms Fe1 and Fe2 are located in an octahedral oxygen environment (the $8f$ Wyckoff position), the third iron atom Fe3 is coordinated by a trigonal prism formed by oxygen atoms (the $4c$ Wyckoff position). The optimized lattice parameters are $a = 2.89$ Å, $b = 10.08$ Å, $c = 15.51$ Å, and $V = 426$ Å³, which is within 3% agreement with the experimental values reported in [6]. Four octahedra connected by common edges in the Fe2–Fe1–Fe1–Fe2 sequence form a slab of width $N = 4$. Iron ions at the Fe3 site create chains along the a axis. The average $\langle \text{Fe–O} \rangle$ bond lengths are $\langle d_{\text{Fe1–O}} \rangle = 2.09$ Å, $\langle d_{\text{Fe2–O}} \rangle = 2.14$ Å, and $\langle d_{\text{Fe3–O}} \rangle = 2.20$ Å. The longest bond length is observed in the Fe₃O₆ prism, implying that this site is occupied by iron ions in the divalent state.

To determine possible magnetic structures of Fe₅O₆, we performed a group-theoretical analysis of the irreducible representations. Any axial-vector configurations in periodic crystals are described as some linear combination of basis vectors of irreducible representations of the parent space group. In this work, we consider only the magnetic structures corresponding to the propagation vector $k = (0, 0, 0)$. The expansion in terms of irreducible representations for $8f$ and $4c$ sites have the form

$$\Gamma(8f) = m\Gamma_1^+ \oplus 2m\Gamma_1^- \oplus 2m\Gamma_2^+ \oplus m\Gamma_2^- \\ \oplus 2m\Gamma_4^+ \oplus m\Gamma_4^- \oplus m\Gamma_3^+ \oplus 2m\Gamma_3^-,$$

$$\Gamma(4c) = m\Gamma_1^- \oplus m\Gamma_2^+ \oplus m\Gamma_2^- \oplus m\Gamma_4^+ \oplus m\Gamma_3^+ \oplus m\Gamma_3^-.$$

According to the Landau theory, we take into account only the magnetic structures corresponding

Table 1. Irreducible representations (IrReps), magnetic space groups, and basis vectors for the $8f$ (Fe1 and Fe2) and $4c$ (Fe3) sites in the case of the $k = (0, 0, 0)$ propagation vector in Fe_5O_6 . The data are given only for the magnetically independent Fe_i atoms, where $i = 1-10$

IrReps/magnetic groups	Basis vectors									
	Fe ₁	Fe ₂	Fe ₃	Fe ₄	Fe ₅	Fe ₆	Fe ₇	Fe ₈	Fe ₉	Fe ₁₀
	Fe1 ($8f$)				Fe2 ($8f$)				Fe3 ($4c$)	
$m\Gamma_1^-/\text{Cm}'c'm'$ (no. 63.465)	0uv	0-uv	0u-v	0-u-v	0uv	0-uv	0u-v	0-u-v	0u0	0-u0
$m\Gamma_2^+/\text{Cm}'c'm'$ (no. 63.462)	0uv	0-uv	0-uv	0uv	0uv	0-uv	0-uv	0uv	00u	00u
$m\Gamma_2^-/\text{Cmcm}'$ (no. 63.461)	u00	-u00								
$m\Gamma_4^+/\text{Cm}'cm'$ (no. 63.464)	0uv	0u-v	0u-v	0uv	0uv	0u-v	0u-v	0uv	0u0	0u0
$m\Gamma_3^+/\text{Cmc}'m'$ (no. 63.463)	u00									
$m\Gamma_3^-/\text{Cm}'cm'$ (no. 63.459)	0uv	0u-v	0-uv	0-u-v	0uv	0u-v	0-uv	0-u-v	00u	00-u

Table 2. Energies of some possible spin configurations corresponding to irreducible representations (IrReps) for the propagation vector $k = (0, 0, 0)$, which are defined relative to the energy of the ground magnetic state (AFM1) for Fe_5O_6

IrReps	$m\Gamma_1^-$	$m\Gamma_2^+$	$m\Gamma_2^-$	$m\Gamma_4^+$	$m\Gamma_3^+$	$m\Gamma_3^-$
Magnetic state	AFM1	FM1	AFM2	FM2	FM3	AFM3
ΔE (meV/f.u.)	0	168	47	78	303	97

to the same irreducible representations, namely: $m\Gamma_1^-$, $m\Gamma_2^+$, $m\Gamma_2^-$, $m\Gamma_4^+$, $m\Gamma_3^+$, and $m\Gamma_3^-$. The irreducible representations and basis vectors for the $8f$ and $4c$ sites are listed in Table 1.

Both collinear and noncollinear spin configurations are possible in Fe_5O_6 . Structures whose basis vectors of irreducible representations ($m\Gamma_2^-$ and $m\Gamma_3^+$) correspond to spin configurations with magnetic moments oriented along the a axis belong to the first type. The basis vectors of the other representations correspond to both collinear and noncollinear orthogonal configurations. In these configurations, the magnetic moments of Fe1 and Fe2 atoms are antiferromagnetically ordered in the bc plane, and the magnetic moments of Fe3 atoms in the chains are ferromagnetically/antiferromagnetically ordered along the b/c axes. The orthogonal spin configurations arise due to the decomposition of the original magnetic system into two, the first of which is represented by octahedrally coordinated iron atoms in $8f$ sites (slabs), the second includes linear chains consisting of iron ions in trigonal prisms ($4c$). In the slabs, an antiferromagnetic ordering of spins along the b ($m\Gamma_2^+$) or c ($m\Gamma_4^+$) axis is observed, with the ferromagnetic component directed along the c or b axis, respectively, or simultaneous antiferromagnetic ordering in the bc plane ($m\Gamma_1^-$, $m\Gamma_3^-$), which suggests a canted spin structure. Magnetic

moments in prisms can be both ferromagnetically ordered along the b ($m\Gamma_4^+$) or c ($m\Gamma_2^+$) axis and antiferromagnetically ordered along the b ($m\Gamma_1^-$) or c ($m\Gamma_3^-$) axis. In this case, the magnetic moments in the chains (Fe3) are orthogonal to the corresponding antiferromagnetic component of the magnetic moments in the slabs (Fe1, Fe2), contributing to the formation of orthogonal ferromagnetic and antiferromagnetic spin configurations.

Based on the above analysis of the irreducible representations, DFT+ U calculations of the total energies of various magnetic structures were performed. For each irreducible representation, the energies of several magnetic structures were calculated, and the magnetic configurations corresponding to the lowest energy for this representation were determined. The results of such calculations are summarized in Table 2. Here, FM and AFM denote the resulting ferromagnetic and antiferromagnetic states, respectively. The orthogonal AFM1 ($m\Gamma_1^-$) structure shown in Fig. 2a is found to have the lowest total energy, consistent with the empirical and crystallographic predictions [12]. In this phase, the magnetic moments in the slabs (Fe1, Fe2) have a large antiferromagnetic component along the c axis and a small antiferromagnetic component along the b axis, leading to the canting of the magnetic moments. The magnetic moments of Fe1 and Fe2 are antiferromagnetically ordered relative to each other.

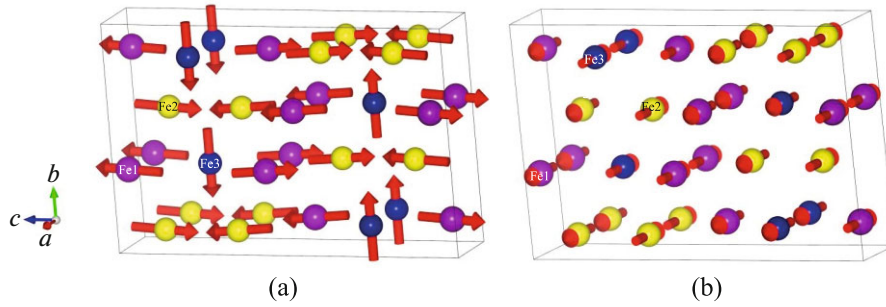


Fig. 2. (Color online) Most energetically favorable magnetic structures of Fe₅O₆: (a) AFM1 ($m\Gamma_1^-$) and (b) AFM2 ($m\Gamma_2^-$) for the vector $k = (0, 0, 0)$. The arrows show the directions of Fe spins in the sites Fe1 (purple), Fe2 (yellow), and Fe3 (blue).

The magnetic moments in Fe3 chains are directed along the b axis and are antiferromagnetically coupled along the c axis. Note that the magnetic moments in the Fe3 chains are orthogonal to the magnetic moments in the slabs. The magnetic moment components at the nonequivalent iron ions (m_x, m_y, m_z) along the crystallographic axes are $m_1 = (0, 0.5, 3.9)\mu_B$, $m_2 = (0, 0.6, 3.8)\mu_B$, and $m_3 = (0, 3.6, 0)\mu_B$ for Fe1, Fe2, and Fe3, respectively.

The second most energetically favorable magnetic structure is the antiferromagnetic configuration AFM2, which corresponds to the irreducible representation $m\Gamma_2^-$. In this structure, the magnetic moments in both slabs and linear chains are directed along the a axis and antiferromagnetically coupled along the c axis (Fig. 2b). The absence of components along the other directions makes this spin configuration collinear. The energy difference between the AFM1 and AFM2 phases is $\Delta E = 47$ meV per formula unit. Thus, in relatively low magnetic fields, one can expect a transition from the noncollinear orthogonal AFM1 structure to the collinear AFM2 one, which corresponds to a 90° rotation of magnetic moments at all nonequivalent sites and can manifest itself in anomalies on magnetization curves and in spontaneous spin-orientation transitions. The spin configuration FM3 (irreducible representation $m\Gamma_3^+$) is the most unfavorable in energy ($\Delta E = 303$ meV/f.u.), suggesting the existence of a high energy barrier, which is required to achieve the complete ferromagnetic order along the a axis. The transition to this state will correspond to the spin-flip transition in the applied magnetic field.

A small canting of magnetic moments in the slabs in the direction of the b axis obtained in theoretical calculations is due to the effect of magnetic chains on the three-dimensional magnetic structure. Magnetically ordered chains are protected by symmetry from the perturbations created by the slabs, but not vice versa [12]. Moreover, our calculations for CaFe₄O₆, where Fe3 atoms are replaced by nonmagnetic cal-

cium atoms, do not reveal any signs of such a canting. We can conclude that the occupation of prismatic sites by a magnetic ion leads to the violation of the collinear antiferromagnetic order in the slabs and to the appearance of canting in the magnetic substructure. Unlike the canting of magnetic moments to the b axis in Fe₄O₅ that was created by the ferromagnetic component of the basis vector of the corresponding irreducible representation, the canting of magnetic moments in Fe₅O₆ corresponds to the antiferromagnetic component of the basis vector due to the symmetry.

Summarizing, we can say that our calculations in this work and in [20] show that the width of the slab N gives rise to the difference in the magnetic ordering of the chains separated by this slab along the c axis. In Fe₅O₆, the magnetic chains formed by Fe3 ions separated by a slab with $N = 4$ are antiferromagnetically ordered, whereas the same chains in Fe₄O₅ separated by a slab with $N = 3$ are ferromagnetically ordered with respect to each other. Thus, according to our DFT calculations for Fe₄O₅ [20] and Fe₅O₆, the antiferromagnetic order in both compounds occurs in slabs, while the resulting magnetic order of the chains in these two compounds will be determined by the slab width N (ferromagnetic at $N = 3$ in Fe₄O₅ and antiferromagnetic at $N = 4$ in Fe₅O₆). The analysis is in full agreement with the hypothesis concerning the generic magnetic structure for iron oxides of the N family put forward in [12].

4. CONCLUSIONS

Combining group-theoretic analysis and DFT+ U calculations, we have determined for the first time the ground magnetic state of the Fe₅O₆ iron oxide. The analysis demonstrated that the ground magnetic state corresponds to the orthogonal ordering of two magnetic subsystems, the first of which is represented by octahedrally coordinated iron atoms in the sites Fe1 (8f) and Fe2 (8f) (slabs) and the second one is formed by chains along the a axis consisting of iron Fe3 ions in trigonal prisms (4c). For the magnetic vector $k =$

(0, 0, 0), the magnetic moments in the slabs are antiferromagnetically ordered along the c axis, while the magnetic moments in the trigonal prisms are directed along the b axis being antiferromagnetically coupled along the c axis. The effect of magnetic chains on the three-dimensional magnetic structure leads to the canted antiferromagnetic ordering in the slabs with a nonzero magnetic moment component along the b axis. The computational results are in good agreement with the generic magnetic structure for the N family iron oxides proposed in [12]. The predicted magnetic structure requires an experimental confirmation.

ACKNOWLEDGMENTS

The calculations were performed using the computer resources of “Complex for Simulation and Processing of Data from Mega-Class Research Facilities,” National Research Center Kurchatov Institute (<http://ckp.nrcki.ru>).

FUNDING

V. Zhandun and N. Kazak acknowledge the support of the Russian Science Foundation (project no. 21-52-12033) and D. Vasiukov acknowledges the support of the Swedish Research Council (project no. 2018-04704).

CONFLICT OF INTEREST

The authors of this work declare that they have no conflicts of interest.

REFERENCES

1. B. Lavina, P. Dera, E. Kim, Y. Meng, R. T. Downs, P. F. Weck, S. R. Sutton, and Y. Zhao, *Proc. Natl. Acad. Sci. U. S. A.* **108**, 17281 (2011).
2. T. Ishii, L. Uenver-Thiele, A. B. Woodland, E. Alig, and T. Boffa Ballaran, *Am. Mineral.* **103**, 1873 (2018).
3. S. V. Ovsyannikov, M. Bykov, E. Bykova, et al., *Nat. Chem.* **8**, 501 (2016).
4. E. Bykova, L. Dubrovinsky, N. Dubrovinskaia, M. Bykov, C. McCammon, S. V. Ovsyannikov, H.-P. Liermann, I. Kuppenko, A. I. Chumakov, R. Ruffer, M. Hanfland, and V. Prakapenka, *Nat. Commun.* **7**, 10661 (2016).
5. R. Sinmyo, E. Bykova, S. V. Ovsyannikov, C. McCammon, I. Kuppenko, L. Ismailova, and L. Dubrovinsky, *Sci. Rep.* **6**, 32852 (2016).
6. B. Lavina and Y. Meng, *Sci. Adv.* **1**, e1400260 (2015).
7. S. V. Ovsyannikov, M. Bykov, S. A. Medvedev, P. G. Naumov, A. Jesche, A. A. Tsirlin, E. Bykova, I. Chuvashova, A. E. Karkin, V. Dyadkin, D. Chernyshov, and L. S. Dubrovinsky, *Angew. Chem. Int. Ed.* **59**, 1 (2020).
8. A. Yang, Q. Qin, X. Tao, S. Zhang, Y. Zhao, and P. Zhang, *Phys. Lett. A* **414**, 127607 (2021).
9. Q.-Y. Qin, A.-Q. Yang, X.-R. Tao, L.-X. Yang, H.-Y. Gou, and P. Zhang, *Chin. Phys. Lett.* **38**, 089101 (2021).
10. S. Maitani, R. Sinmyo, T. Ishii, S. I. Kawaguchi, and N. Hirao, *Phys. Chem. Miner.* **49**, 11 (2022).
11. S. V. Ovsyannikov, M. Bykov, E. Bykova, et al., *Nat. Commun.* **9**, 4142 (2018).
12. D. M. Vasiukov, G. Khanal, I. Kuppenko, G. Aprilis, S. V. Ovsyannikov, S. Chariton, V. Cerantola, V. Potapkin, A. I. Chumakov, L. Dubrovinsky, K. Haule, and E. Blackburn, *arXiv: 2207.14111* (2022).
13. K. Hikosaka, R. Sinmyo, K. Hirose, T. Ishii, and Y. Ohishi, *Am. Mineral.* **104**, 1356 (2019).
14. S. Layek, E. Greenberg, S. Chariton, M. Bykov, E. Bykova, D. M. Trots, A. V. Kurnosov, I. Chuvashova, S. V. Ovsyannikov, I. Leonov, and G. Kh. Rozenberg, *J. Am. Chem. Soc.* **144**, 10259 (2022).
15. E. J. W. Verwey, *Nature (London, U.K.)* **144**, 327 (1939).
16. K. H. Hong, G. M. McNally, M. Coduri, and J. P. Attfield, *Z. Anorg. Allgem. Chem.* **642**, 1355 (2016).
17. K. H. Hong, A. M. Arevalo-Lopez, M. Coduri, G. M. McNally, and J. P. Attfield, *J. Mater. Chem. C* **6**, 3271 (2018).
18. K. H. Hong, A. M. Arevalo-Lopez, J. Cumby, C. Ritter, and J. P. Attfield, *Nat. Commun.* **9**, 2975 (2018).
19. K. H. Hong, E. Solana-Madruga, M. Coduri, and J. P. Attfield, *Inorg. Chem.* **57**, 14347 (2018).
20. V. S. Zhandun, N. V. Kazak, I. Kuppenko, D. M. Vasiukov, X. Li, E. Blackburn, and S. G. Ovchinnikov, *Dalton Trans.* **53**, 2242 (2024).
21. G. Kresse and J. Furthmuller, *Phys. Rev. B* **54**, 11169 (1996).
22. G. Kresse and D. Joubert, *Phys. Rev. B* **59**, 1758 (1999).
23. P. Perdew, K. Burke, and M. Ernzerhof, *Phys. Rev. Lett.* **77**, 3865 (1996).
24. H. J. Monkhorst and J. D. Pack, *Phys. Rev. B* **13**, 5188 (1976).
25. S. L. Dudarev, G. A. Botton, S. Y. Savrasov, C. J. Humphreys, and A. P. Sutton, *Phys. Rev. B* **57**, 1505 (1998).
26. J. Rodriguez-Carvajal, *Phys. B (Amsterdam, Neth.)* **192**, 55 (1993).
27. K. Momma and F. Izumi, *J. Appl. Crystallogr.* **44**, 1272 (2011).

Translated by K. Kugel

Publisher’s Note. Pleiades Publishing remains neutral with regard to jurisdictional claims in published maps and institutional affiliations.